 doi:10.20944/preprints202107.0408.v1

Article

Analysis of Tidal Accelerations in the Solar System and in Extra-solar Planetary Systems

Klaus Paschek [1+], Arthur Roßmann [1], Michael Hausmann [1,*] and Georg Hildenbrand [1,*]

[1] Heidelberg University, Department of Physics and Astronomy, Kirchhoff-Institute for Physics, Im Neuenheimer Feld 227, 69120 Heidelberg, Germany; KP: paschek@mpia.de, AR: a.rossmann@stud.uni-heidelberg.de
[+] present address: Max-Planck-Institute for Astronomy, Königstuhl 17, 69117 Heidelberg, Germany
* Correspondence: MH: hausmann@kip.uni-heidelberg, Tel: +49-6221-549824; GH: hilden@kip.uni-heidelberg;

The article is presenting simulations for tidal accelerations in multi-body planetary systems under the precondition of having only few physical and orbital parameters experimentally available. Tidal acceleration vectors were calculated under missing most orbital parameters for the solar system as calibration standard and the TRAPPIST-1 system as an extrasolar example.

Abstract: Volcanism powered by tidal forces inside celestial bodies can provide enough energy to keep important solvents for living systems in the liquid phase. Moreover, tidal forces and their environmental consequences may strongly influence habitability of planets and other celestial bodies and may result in special forms of live and living conditions. A prerequisite to calculate such tidal interactions and consequences is depending on simulations for tidal accelerations in a multi-body system. Unfortunately, from measurements in many extrasolar planetary systems only few physical and orbital parameters are well enough known for investigated celestial bodies. For calculating tidal acceleration vectors under missing most orbital parameter exactly, a simulation method is developed that is only based on a few basic parameters, easily measurable even in extrasolar planetary systems. Such a method as being presented here, allows finding a relation between the tidal acceleration vectors and potential heating inside celestial objects. Using values and results of our model approach to our solar system as a "gold standard" for feasibility allowed us to classify this heating in relation to different forms of volcanism. This "gold standard" approach gave us a classification measure for the relevance of tidal heating in other extrasolar systems with a reduced availability of exact physical parameters. We would help to estimate conditions for the identification of potential candidates for further sophisticated investigations by more complex established methods like viscoelastic multi-body theories. As a first example, we applied the procedures developed here to the extrasolar planetary system TRAPPIST-1 as an example to check our working hypothesis.

Keywords: tidal forces, numeric simulation, acceleration vectors, multi-planetary system, extrasolar planets/planet systems

1. Introduction

In the last decades, many objects in the solar system have been identified with liquid oceans powered by tidal heating. Well-known examples are (J1) Io [designation (J1) given in this paper for distinction from asteroid (85) Io], Europa, Enceladus and Ganymede among a lot more. In principle tidal heating or in more general considerations tidal interactions happen in all planetary systems known in the universe. An additional specialty in many extrasolar planetary systems, especially in those of the numerous M and K stars, is the very great proximity of planetary objects to each other [1-3]. This might already result in an influence the planetary objects have on each other. These additional effects based on multi-body contributions to tidal interactions were so far only rarely considered, especially since all relevant physical parameters required for complex modelling were not available for many extrasolar systems.

 doi:10.20944/preprints202107.0408.v1

Without denying the need for deep and detailed analyses based on complex theoretical approaches as for instance the successful viscoelastic multi-body theories, it may be of advantage to have a rough calculation procedure whenever the measured data availability does not sufficiently satisfy the theories´ requirements. This may offer a glimpse on potential systems of interest in advance by a model in which mainly distances between the objects, *R*, *e*, masses and the orbital elements are used. To include the possible mutual multi-planetary influences mentioned above, the forces of all objects on each other have to explicitly be considered. Since tidal interactions from gravity forces up to complex tidal heating models require in a first step an approach to estimate accelerations and the mutual interaction of multi-bodies, we developed in this first approach a procedure considering both requirements, i.e., a simulation of a time course of variations of the resulting tidal accelerations under *multi-body conditions* and with a *minimalistic set of experimental physical parameters*. This has been achieved by computing all acceleration vectors affecting every object in order to identify planetary systems which are potentially tidal driven. The model was first applied on our solar system as a "gold standard" to determine whether this is sufficient to identify candidates for tidal interactions. Our solar system is the best test candidate, because a comparison to precise measurements and models developed for the many objects in the solar system can be made. Often space probes have visited these objects and accurate investigations have been done so that the results can be used in some way as a standard to classify other systems so far not investigated in such great details. This may even allow an assessment of whether a certain value found in the model may favor liquid solvents, cryo- or even siliceous volcanism inside the object.

In addition, some aspects in the evolution of the eccentricity *e* over time have been investigated in this approach. In a final step, this approach has been applied to an extrasolar planetary system, namely TRAPPIST-1. All planets known for this system are included. We further present our results for a simplified version of our simulation, using a smaller set of orbital elements. We compare this simplified version to the original one and outline how this simplified version could be applicable to other extrasolar planetary systems for which usually only a smaller set of orbital elements is known with acceptable accuracy. This could give a first estimate for the potential significance of tidal influences in other less well-known extrasolar systems. Finally, we discuss this new developed pre-screening method for extrasolar systems, as well as further findings and implications for objects in our solar system.

2. Materials and Methods

2.1. Tidal accelerations

Tracking the orbital motion of celestial bodies based on their orbital elements allows to calculate the positions of the object for discrete time steps and to determine the three-dimensional distance vectors between the objects. Using a minimalistic set of physical and geometrical parameters of the objects, we calculate the tidal acceleration vectors acting on the surface of one object. After this step, for easier evaluation, the distance vectors were normalized and multiplied by the absolute value of the tidal acceleration *A* acting on the surface of the influenced object facing the influencing objects following Eq. (1).

$$A = \frac{GM}{r^2}\left(\frac{1}{\left(1-\frac{R}{r}\right)^2} - 1\right) \quad (1)$$

M is the mass of an influencing object; *r* is the distance between the objects, and *R* the radius of the influenced object. Considering also influences of a changing orbit, we use *e*

(eccentricity), as well as parameters for the orientation of the objects in space and amongst each other, as e.g. i (inclination) and Ω (longitude of the ascending node). This allows a computation of acceleration vectors in 3D caused by every object in the system on the investigated one. Adding up these acceleration vectors takes into account, that the tidal effects caused by several objects can intensify or partially cancel each other out, due to the different orientations of the tidal acceleration vectors acting on the objects. Determining the vector difference between these "total", summed up tidal accelerations for the different time steps also gives a rough estimate of the deformation of the objects and may serve therefore as an indicator for the possible tidal heating on their inside.

2.2. Data

To simulate the motion of the planets, moons, asteroids and comets in the solar system one needs the orbital elements of these objects. The data for the planets and their moons are obtained from the *Solar System Bodies Archive* [4] and the data for the asteroids and comets is gathered from the *JPL Small-Body Database Search Engine* [5]. Although being of general importance masses are only listed for a small fraction of asteroids and comets. To give a rough estimate for the missing masses, we calculate the mean density of the known objects, suppling masses using their radius under the assumption of a spherical shape. Based on this mean density and its standard deviation, an estimate for the masses of the other objects is obtained using their radii. The mean density gives a mean mass estimate and the mean density plus/minus the standard deviation gives a maximal/minimal mass estimate. With these values the tidal accelerations for each of the three masses (maximum, mean, minimum) are computed.

We also include trans-Neptunian-objects (TNOs) in our simulation. The data for their physical and orbital properties are taken from various publications listed in the appendix in Table 2. For some cases, the given values diverge. We only include TNOs for which the accuracy of the given data seems reasonable: errors of values within a publication < 30% or deviations between values of publications < 30%. If several value sources for one object were available, we use the mean value of these data. In the column 'moons' an asterisk (*) denotes that a moon is known for this TNO but not included in the simulation because of missing or inaccurate data. There are even more multi-body systems like e.g. (42355) Typhon - (42355) Typhon I Echidna. Due to lack of (unambiguous) data (79360) Sila-Nunam (1997 CS29), (38083) Rhadamanthus (1999 HX11), (15810) Arawn (1994 JR1), (28978) Ixion (2001 KX76), (420356) Praamzius (2012 BX85), (53311) Deucalion (1999 HU11) and many more are not included either. If a value is not given in the publications, the data from the JPL database is used or the mass is derived as mentioned above. Mass and radius of the sun are taken from [6].

Tidal accelerations are only computed if the radius of the influenced object is larger than 75 km. Since the radius is also part of Eq. (2) one also expects low tidal accelerations for these objects. Objects with a radius smaller than 75 km, however, are included in the influencing objects. For comets, we include only the biggest known objects with a radius around 30 km to test, if there could be some tidal potential.

Data used in the simulation of the extrasolar planetary system TRAPPIST-1 is taken for the central star from [7] for mass and radius and for the planets from [8] for masses, semi-major axes and eccentricities; from [9] for mean angular motions and radii and from [9, 10] for inclinations.

2.3. Simulation of orbital motion

The orbital elements are the semi-major axis a, the eccentricity e, the longitude of the ascending node Ω, the inclination i, the argument of periapsis ω, the mean anomaly at a given epoch M_0 and the mean orbital motion n. For the calculation of the three-dimensional distance vectors, the coordinates of all objects have to be transformed into a single Cartesian coordinate system. As the uniform system, the Cartesian helio-

 doi:10.20944/preprints202107.0408.v1

centric ecliptic system is chosen with the sun at the origin and the orbital plane of the Earth as the x-y-plane with the x-axis pointing to the vernal equinox. Kepler's equation is solved to get the polar coordinates of the elliptic orbit, convert them to Cartesian coordinates and then rotate the orbital plane using the other orbital elements with respect to the ecliptic.

Since the orbital elements of the moons are in reference to their central planet/object, one has to shift their coordinates by those of the central object. The mutual influence of the moons on their orbital motion, in the solar system especially for moons around gas giants, leads to a precession of the orbits and makes it necessary to introduce a new reference plane for some moons, called the Laplace plane. This plane has two additional orbital elements, two angles changing in time, to emulate this precession in a linear approximation. For the outer moons of the gas giants in the solar system this precession is partly caused by the mutual influence of the outer moons of different planets. Some of the inner moons orbit close to the equatorial plane of their gas giant and therefore use this plane as reference, which gives two angles as additional orbital elements, too. Sometimes, these additional angles are in reference to the equatorial plane of the Earth and one must include an additional rotation about the angle of the obliquity of the Earth.

You can find the code for the simulation written in C++ under the following link: https://www.kip.uni-heidelberg.de/biophysik/software/tidal_accelerations. You need C++11 standard and the library "Eigen" [11] for compiling.

In order to find an appropriate time window for the simulation of the orbital motion and the resulting tidal accelerations, we choose conjunctions of the planets, since the mutual influence of the moons of different planets, as mentioned above, and therefore the tidal influence should then be maximal. In May 2000, the planets Mercury, Venus, Earth, Mars, Jupiter and Saturn were located in a relatively small angular segment seen from the sun. So, it makes sense to simulate around this time point, because the planets are getting very close to each other and may have the highest accelerations on each other. To include the approaching of the planets to this situation, we start our simulation at 1.1.1950 12 h UT. Around May 2492 almost the same conjunction will occur, so we choose a time period of 600 years for the simulation to include this conjunction as well.

Since one can only simulate for discrete time steps, a reasonable value for each time step has to be determined. For this we consider the orbital periods of the objects in the solar system. The planets have orbital periods of barely over three months for Mercury to 165 years for Neptune or rather 248 years for the dwarf planet Pluto. In contrast to that, the periods of the moons of the gas giants range from a quarter of a day for the inner ones up to a few years for the outer ones. Among the asteroids, (101955) Bennu orbits in about 1.20 years, while (4) Vesta takes about 3.63 years. TNOs have orbital periods up to 497.5 years for (90377) Sedna. Comets are strongly diverging, 5.37 years for the Jupiter-family comet 10P/Tempel and 2640 years for (C/1995 O1) Hale-Bopp.

As the asteroids in the main belt have at least a period of about one year, we choose a step size of 90 days, in order to have at least four points on the orbit for these asteroids. Also, the four inner terrestrial planets, all asteroids, comets and TNOs are simulated using this step size, resulting in $600\ years / 0.25\ years = 2{,}400$ iterations.

The first interesting moon according to its size is the Saturn moon Mimas with an orbital period of about one day. Again, we choose a quarter of this as our step size and iterate 2,400 times resulting in a total time period of 600 day In this way, the simulations are carried out for the moons and the terrestrial central objects, Earth, Mars, Pluto and the TNOs Eris and Haumea, to get a more detailed insight into the tidal influence of their moons. To include the conjunction around May 2000, we start the simulation on May 1999 for this smaller step size.

As the orbital periods of the planets in the TRAPPIST-1 system are relatively close to each other with 1.5 to 18.8 days we chose a smaller step size of 0.1 days. Going for 1,800 iterations we get almost 10 orbits for the outermost planet.

Preprints (www.preprints.org) | NOT PEER-REVIEWED | Posted: 19 July 2021 doi:10.20944/preprints202107.0408.v1

Converting the distance vectors into tidal acceleration vectors using Eq. (1), we obtain a vector set for every object pointing to the other influencing objects. Since for many celestial bodies we have three values for the mass (mean, minimal and maximal guessed mass), we obtain a triple of these tidal accelerations for every time step using these different mass values in calculation, respectively. If the mass is given for an object, we only use this single value so that we end up with identical tidal acceleration vectors instead of different vectors in the triple.

Adding up these vectors related to the influencing objects for a certain time step and taking the norm results in the tidal acceleration A_{total}. Note that this takes the three-dimensional orientation of the vectors into account, as the tidal influences of the many objects may (partially) enhance or reduce each other. In addition, we calculate the vector difference of the total acceleration vectors A_{total} by subtracting them from each other for two consecutive time steps. We call the norm of this difference value ΔA_{total}. This represents the change of the tidal acceleration vectors including the change in the orientation. Our idea is that this could give a rough estimation of a deformation of the object caused by the change in the tidal forces.

Eq. (1) can be approximated for $R \ll r$ by

$$A \approx \frac{2GMR}{r^3} \tag{2}$$

Using Δt for the step size in the simulation in days, mean angular motion n, and approximating $(\Delta A / \Delta t)$ by An, we obtain

$$A\frac{\Delta A}{\Delta t} \approx A^2 n \approx \frac{4G^2M^2R^2n}{r^6} \tag{3}$$

Since parts of the simulation use different step sizes Δt, this product also guarantees the comparability of the values with each other (e.g., moons often complete an orbit faster than a planet).

To reduce the amount of resulting data for each object we apply a pre-screening to find 10 objects with the greatest influence. In addition, we search for 10 objects with the greatest fluctuations in their influence, since this is interesting in connection to the potential for deforming the interior of the celestial body.

To visualize the tidal accelerations, we generate for every object a series of bar charts applying the values over the discrete time steps. The uppermost graph contains the individual contributions of the influencing objects stacked logarithmically, the second one the resulting A_{total}, the third one ΔA_{total} and the last one at the bottom $A_{total} \cdot (\Delta A_{total} / \Delta t)$. Every bar in these charts consists of three sub-bars, including the value of the tidal acceleration calculated using the minimal, mean and maximal mass guess from left to right (Figures. 1-4, 8- 10).

You can find the Python3 script generating the plots using the data resulting from the C++ simulation also in the file package under the above-mentioned link.

3. Results

A typical example is shown in Figure 1, in which all the strongest of the tidal influences acting on the Jovian moon Ganymede can be seen. As expected, Jupiter has the biggest contribution to the tidal acceleration since it is the largest mass around. Second by contribution are the other Galilean moons, but already in the range of at least 4 orders of magnitude smaller. Their periodicities reflect very well the orbital resonances of these moons. Moreover, other Jovian moons appear in the objects causing large fluctuations as expected. Figure 2 shows as another example, the tidal influence acting on (4) Vesta being dominated by the sun and its influence is also in the range of 3 to 4 orders of magnitude higher than those by planets nearby the main belt and other asteroids within this belt. The results presented in these two figures indicate some general characteristics of our

Preprints (www.preprints.org) | NOT PEER-REVIEWED | Posted: 19 July 2021 doi:10.20944/preprints202107.0408.v1

computed tidal accelerations and the expected tidal influences for celestial bodies in our solar system.

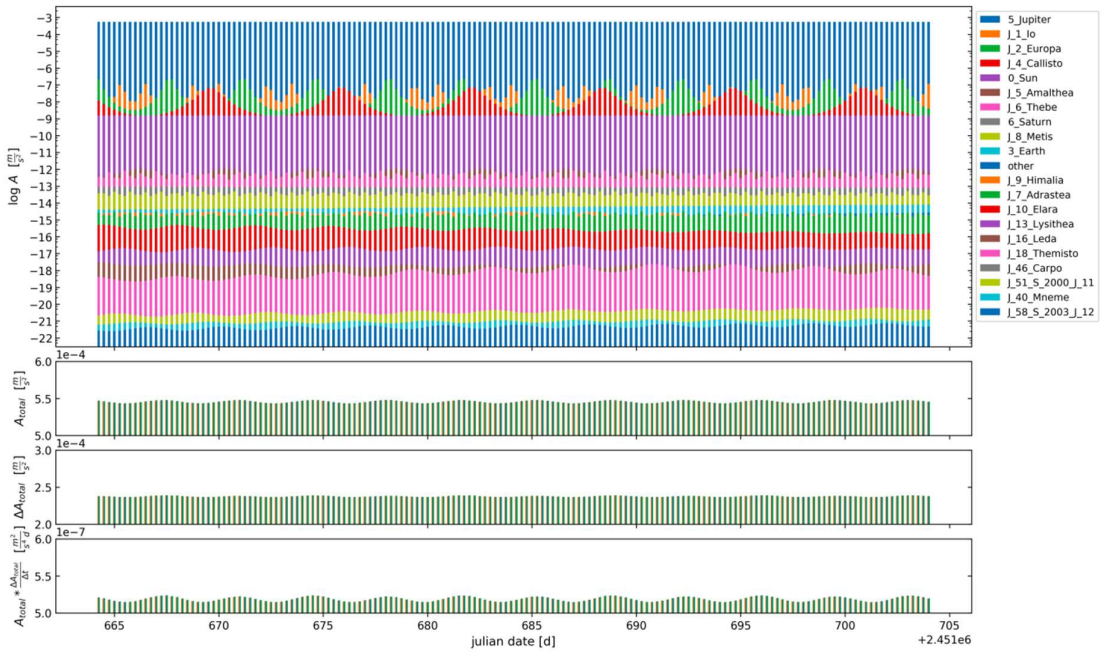

Figure 1. Tidal accelerations acting on Jovian moon Ganymede using the version of the simulation with full orbital elements; Δt = 0.25 days (d). A denotes the individual tidal accelerations caused by other objects. The ordering of the legend is the same as in the uppermost plot with the strongest contribution at the top and the weakest at the bottom. A_{total} denotes the norm of the vector addition of all individual contributions. ΔA_{total} denotes the norm of the vector difference of A_{total} for two consecutive time steps.

Not only the sun and planets influence (4) Vesta, also the Moon and other asteroids like (1) Ceres, (9) Metis or (85) Io generate tidal accelerations that change dramatically over time. Since all these objects including (4) Vesta itself are relatively small, light and/or too far apart, the absolute values of $A_{total} \cdot (\Delta A_{total} / \Delta t)$ are too small to be interesting enough in the context of tidal heating. Nevertheless, this shows the potential of asteroids for tidal heating besides moons around large gas giants. One can see in Figure 2 that the course of ΔA_{total} follows the course of A_{total} in general. This can be explained by the fact that the sun dominates and ΔA_{total} mostly just corresponds to the change of the orientation of A_{total} caused by the orbital motion of (4) Vesta around the sun.

Results for the three-body system Haumea in the Kuiper belt as given in Figure 3 are very interesting in this context, because the orbital planes of the two moons around Haumea are tilted towards each other due to very different inclinations. In this graph (Figure 3), the effect of non-coplanar orbital planes can be nicely seen: The charts showing A_{total} and also ΔA_{total} differ clearly, because the orientations of the tidal acceleration vectors become important in such a tilted system. This contrasts with (4) Vesta where the effects of the moons are strong enough to dominate ΔA_{total} . For objects orbiting close to their central object it is interesting to check if A_{total} and ΔA_{total} differ significantly. This does not only mean a change of the orientation caused by the orbital motion around the central object contributing to a deformation of the influenced object over time. Objects orbiting close to their central object are often tidally locked, i.e., they are always showing the same side to the central object so that only a change in the orientation of the tidal acceleration vector caused by the orbital motion contributes to ΔA_{total}.

Preprints (www.preprints.org) | NOT PEER-REVIEWED | Posted: 19 July 2021 doi:10.20944/preprints202107.0408.v1

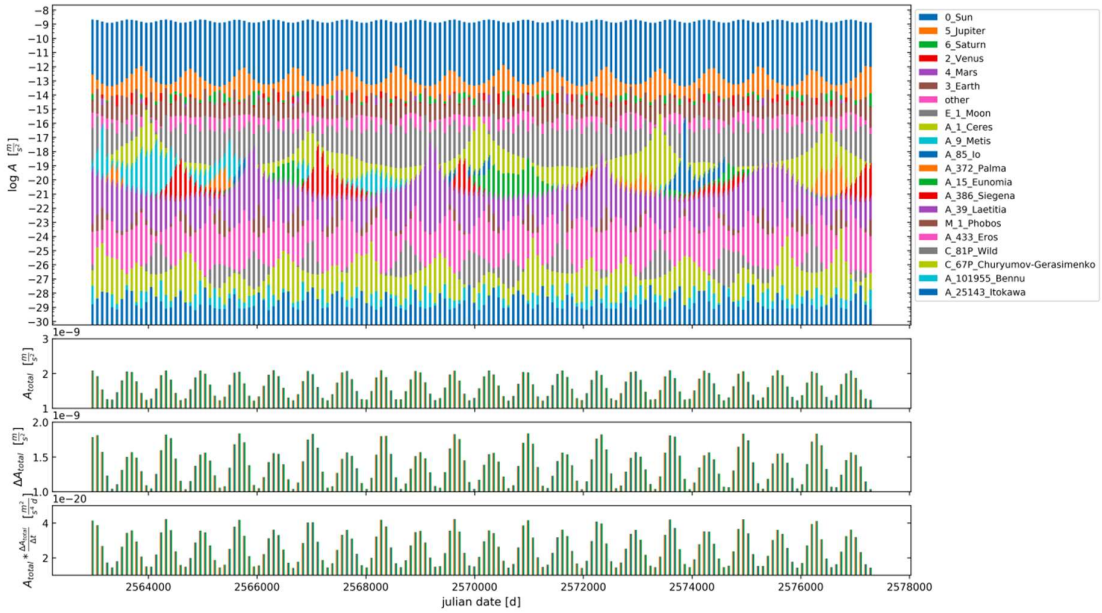

Figure 2. Tidal accelerations acting on main belt asteroid (4) Vesta using the version of the simulation with full orbital elements; Δt = 90 days. A denotes the individual tidal accelerations caused by other objects. The ordering of the legend is the same as in the uppermost plot with the strongest contribution at the top and the weakest at the bottom. A_{total} denotes the norm of the vector addition of all individual contributions. ΔA_{total} denotes the norm of the vector difference of A_{total} for two consecutive time steps.

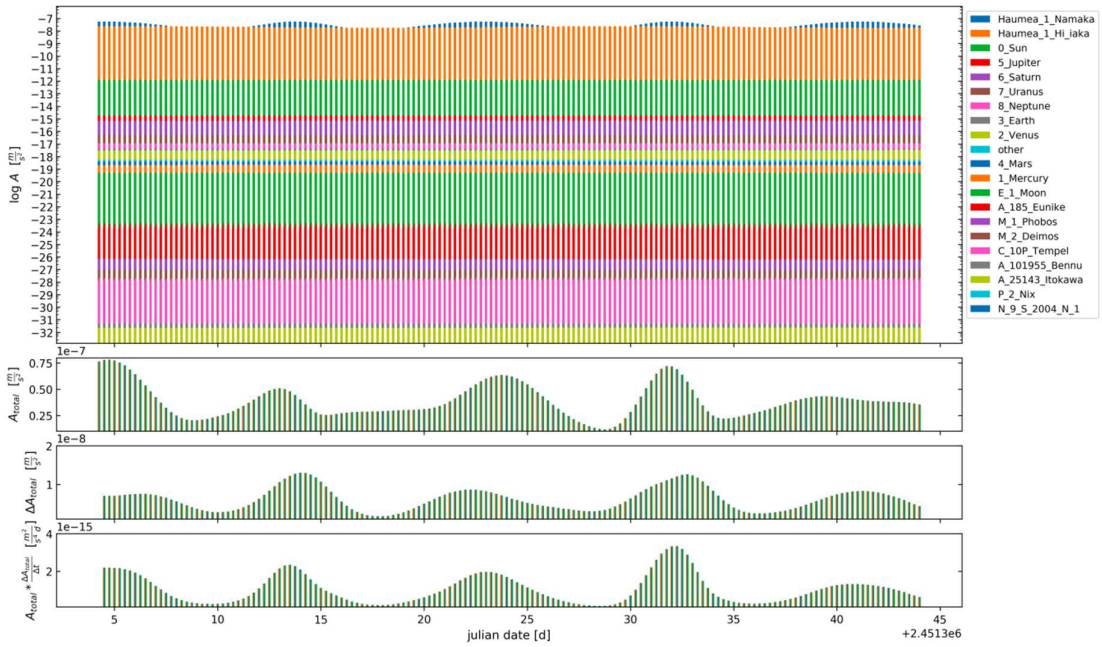

Figure 3. Tidal accelerations acting on TNO (136108) Haumea using the version of the simulation with full orbital elements; Δt = 0.25 days. A denotes the individual tidal accelerations caused by other objects. The ordering of the legend is the same as in the uppermost plot with the strongest contribution at the top and the weakest at the bottom. A_{total} denotes the norm of the vector addition of all individual contributions. ΔA_{total} denotes the norm of the vector difference of A_{total} for two consecutive time steps.

Preprints (www.preprints.org) | NOT PEER-REVIEWED | Posted: 19 July 2021 doi:10.20944/preprints202107.0408.v1

In general, it can be said that among those celestial bodies investigated, TNOs in possession of moons exhibit exceptionally strong tidal influence. In, e.g., [2512] also a huge potential for tidal heating within these TNOs is described. Multi-body TNO systems often consist of relatively large objects orbiting each other in short distance and have, in comparison with solar system planets and moons, quite uncommon values for their orbital elements. Nevertheless, as the accuracy or availability of orbital and physical data for TNOs is in general not very satisfying, especially for TNOs with moons, a (more precise) determination of these parameters could be very interesting for a more detailed evaluation of tidal heating.

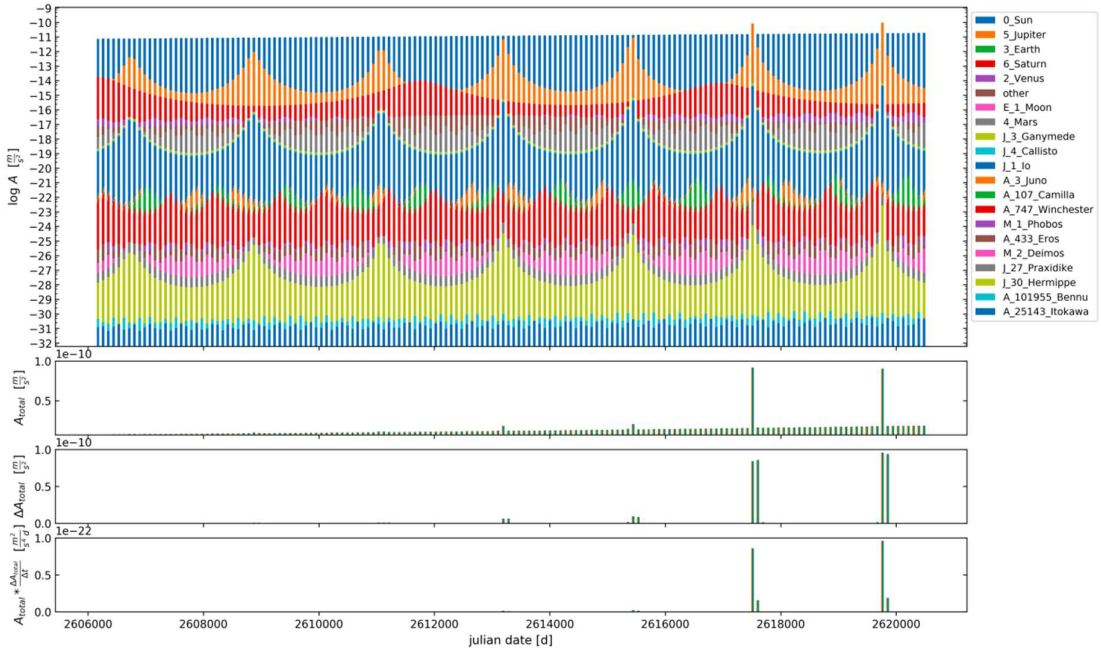

Figure 4. Tidal accelerations acting on comet C/1995 O1 (Hale-Bopp) using the version of the simulation with full orbital elements; Δt = 90 days. A denotes the individual tidal accelerations caused by other objects. The ordering of the legend is the same as in the uppermost plot with the strongest contribution at the top and the weakest at the bottom. A_{total} denotes the norm of the vector addition of all individual contributions. ΔA_{total} denotes the norm of the vector difference of A_{total} for two consecutive time steps.

As the model gives a complete three-dimensional simulation evolving over time, rare and only occasionally occurring encounters of generally not associated objects are more easily revealed. This is especially interesting for comets and some asteroids that travel across the inner and outer regions of the solar system due to their high eccentricities. In Figure 4, the flyby of the comet C/1995 O1 (Hale-Bopp) past Jupiter is shown. The tidal influence increases significantly as Hale-Bopp approaches Jupiter. The tidal accelerations are nevertheless small and the considered parameters are many orders of magnitude below those of objects shown above. This may be mainly due to the small size of Hale-Bopp but could become interesting for bigger asteroids or comets.

Figure 5 gives an overview over the celestial bodies showing the largest tidal accelerations in the solar system. $\{A_{total} \cdot (\Delta A_{total} / \Delta t)\}_{max}$ is the maximal value found for the celestial object over all time steps.

In Figures 6 and 7, volcanism of differently sized objects is discussed in relation to the maximal value $\{A_{total} \cdot (\Delta A_{total} / \Delta t)\}_{max}$. Celestial bodies marked by orange triangles show signs of at least former volcanism, meaning that these objects certainly had volcanism in the past and might even be faintly igneous today. Data of the space probe MESSENGER shows signs of siliceous flood volcanism and other volcanic features on Mercury [13, 14]. Venus shows multiple signs for former and maybe still present volcanism. The Monitoring Camera of the space probe Venus Express [15], numerical simulations [16], and other investigations [17, 18, 19] find hints/evidence for volcanism. It is

Preprints (www.preprints.org) | NOT PEER-REVIEWED | Posted: 19 July 2021 doi:10.20944/preprints202107.0408.v1

reasonably certain that Mars used to be volcanic in the past (e.g. Olympus Mons) and maybe still is today. Also our Moon shows signs for former [20] volcanism and seismic measurements during the Apollo missions indicate present volcanism [21]. This subgroup is presented just for orientation, as again one must consider for these huge objects that radioactive heating and stored accretion energy strongly contribute besides tidal interactions to volcanism.

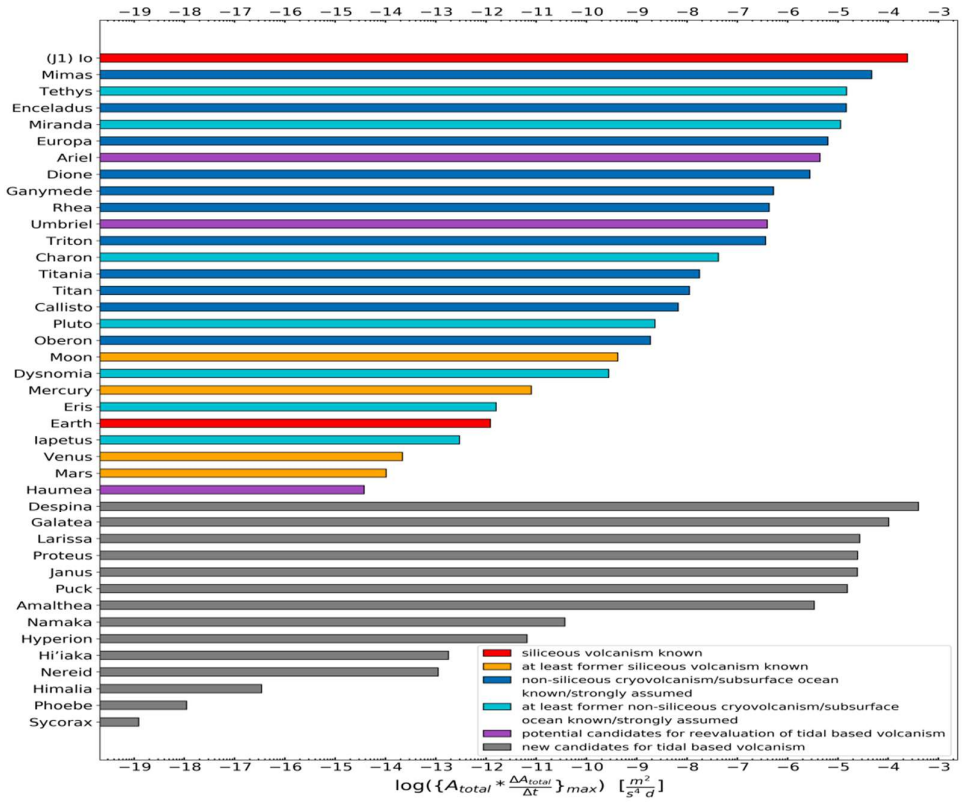

Figure 5. Overview over the celestial objects showing the largest tidal accelerations in the solar system. The version of the simulation with full orbital elements is used. Color-coded is what is known about volcanism on these objects.

As may be already seen from Figure 6, if $\{A_{total} \cdot (\Delta A_{total} / \Delta t)\}_{max}$ is larger than 10^{-15} $[m^2/s^4d]$ and R larger than 200 km, volcanism is known for all objects in the solar system. This general observation makes no assumptions on the power sources of this volcanism. For larger R, this may be more based on radioactive decay or stored accretion energy; for smaller R, this points more towards the direction of tidal heating. Most planets with at least former volcanism known, are below 10^{-10} $[m^2/s^4d]$ and above 10^{-15} $[m^2/s^4d]$, but have higher R values. The probably most interesting new objects exposed to higher gravitational forces found by this simulation can be seen in the upper left corner of the diagram with $\{A_{total} \cdot (\Delta A_{total} / \Delta t)\}_{max}$ larger than 10^{-6} $[m^2/s^4d]$ but R smaller than 200 km. New considerations may also be taken for all other objects shown, even if they are not inside of the boundaries as the objects already described.

Preprints (www.preprints.org) | NOT PEER-REVIEWED | Posted: 19 July 2021 doi:10.20944/preprints202107.0408.v1

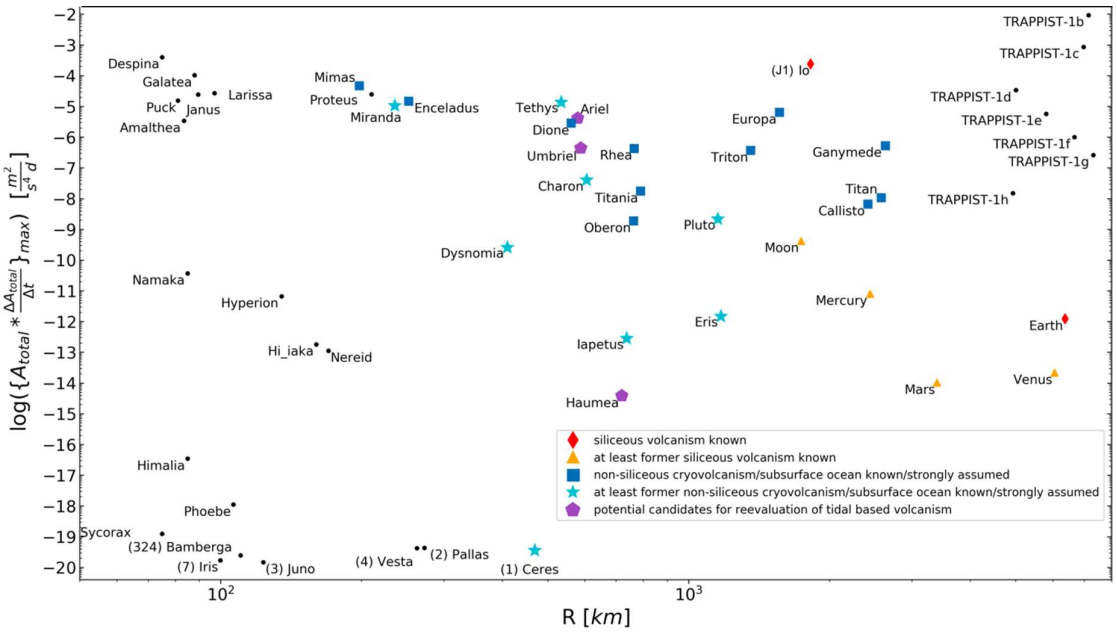

Figure 6. Maximal tidal accelerations against radius of celestial objects in the solar system and the TRAPPIST-1 planetary system. The version of the simulation with ***full orbital elements*** is used. Color-coded is what is known about volcanism on these objects.

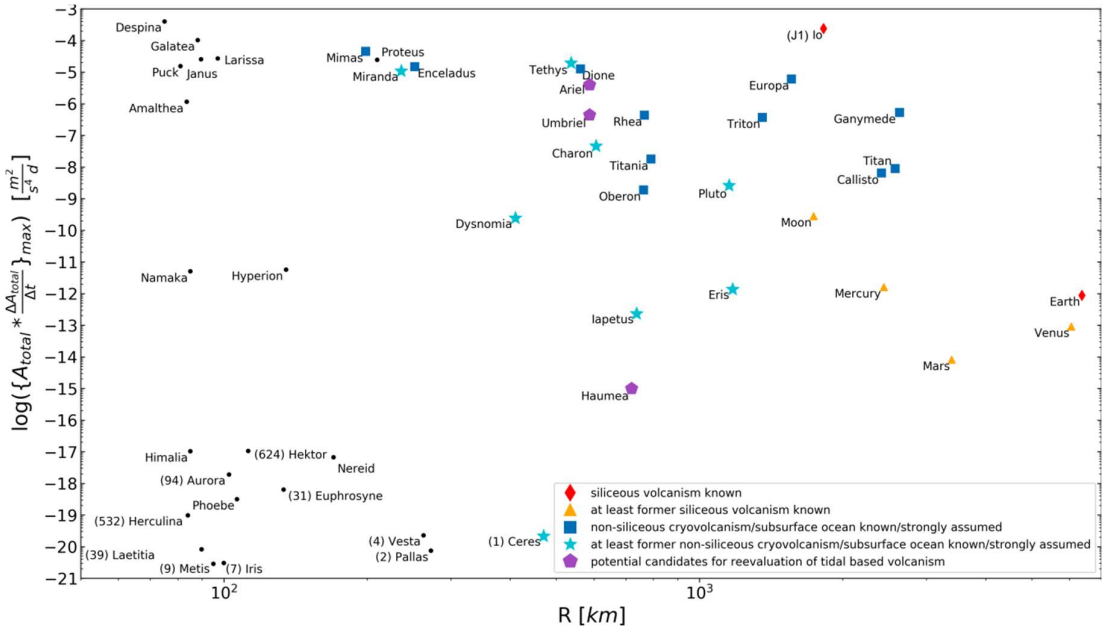

Figure 7. Maximal tidal accelerations against radius of celestial objects in the solar system using the version of the simulation with ***simplified orbital elements.*** Color-coded is what is known about volcanism on these objects.

As mentioned above, for objects in extrasolar planetary systems, very often only a small fraction of their properties and parameters are available. Even orbital elements may be missing or vague. Thus, the application of our simulations is running into uncertainties. To investigate the effect of neglecting some orbital elements on the results of our model, we repeated our whole full simulation by setting e, Ω, i, ω and M_0 to zero so that only a, n, M and R were remaining which often may be the only well-known parameters for objects in an extrasolar planetary system. The new results based on this simplified

Preprints (www.preprints.org) | NOT PEER-REVIEWED | Posted: 19 July 2021 doi:10.20944/preprints202107.0408.v1

simulation are given in Figure 7. Only small deviations were found between the two versions (Figure 7 vs. Figure 6) of the simulation. This may be mostly caused by neglecting the eccentricity e (as been seen in pre-simulations when testing the algorithm, data not shown). The similarity of Figures 6 and 7 shows that the simplified version of the simulation with a smaller set of orbital elements, does not change the resulting tidal accelerations significantly. Thus, the simplified version could be very applicable to estimate the potential significance of tidal influences in extrasolar planetary systems, especially the ones with poorly known or many unknown orbital elements. In general, the deviations are reasonably small and therefore our approach may be considered stable enough to provide an estimate for the tidal interaction and the heating potential in extrasolar planetary systems, even if not all parameters are known. An example is given in Figure 8 for Haumea, where even with strong influences from its orbital planes, the course of the values changes, thereby remaining in the same order of magnitude.

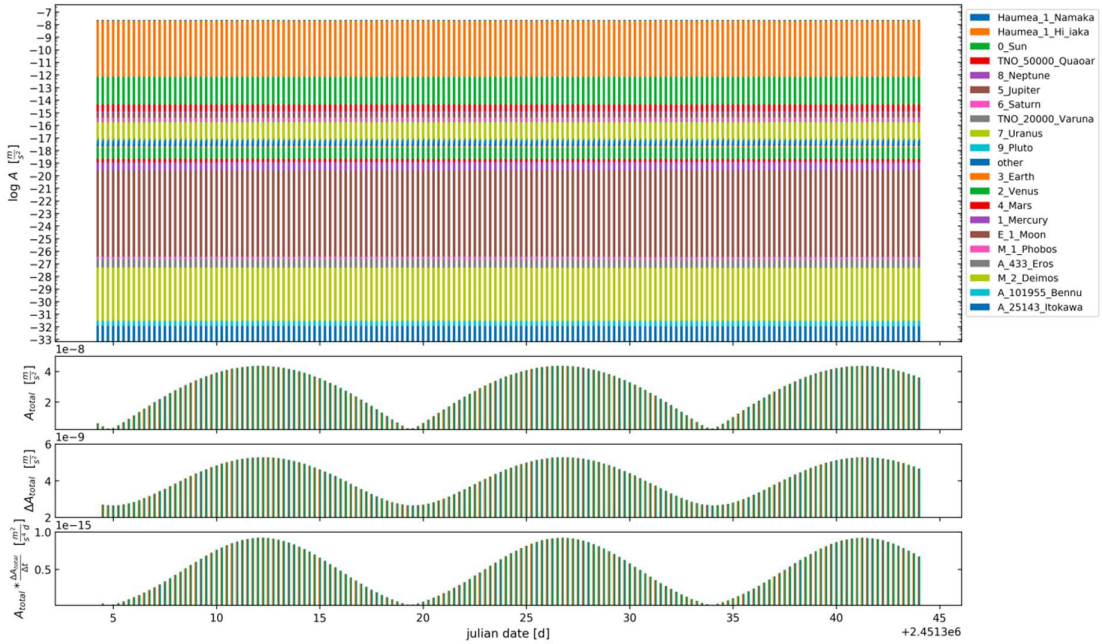

Figure 8. Tidal accelerations acting on TNO (136108) Haumea using the version of the simulation with simplified orbital elements; Δt = 0.25 days. A denotes the individual tidal accelerations caused by other objects. The ordering of the legend is the same as in the uppermost plot with the strongest contribution at the top and the weakest at the bottom. A_{total} denotes the norm of the vector addition of all individual contributions. ΔA_{total} denotes the norm of the vector difference of A_{total} for two consecutive time steps.

.

In the case of special objects where uncertainties are present, the bar histograms of tidal accelerations may give new insights for future improved modelling. As an example of the solar system, the two Uranian moons Ariel and Umbriel are shown. Little energy transfer from their central planet is assumed, but periodic mutual tidal influences of the moons seem to peak over 10^{-7} m/s^2 for A_{total} nearly all three days (Figure 9). This shows that also other objects orbiting the central object can provide the leading important tidal influence. This is a key new feature of the model presented here. We can see (e.g., bottom panel of Figure 9) that referring all calculations to the central object only, might underestimate the potential of tidal influences by other objects present in the system. This example may justify our complex multi-body approach in case of special planetary systems.

Preprints (www.preprints.org) | NOT PEER-REVIEWED | Posted: 19 July 2021 doi:10.20944/preprints202107.0408.v1

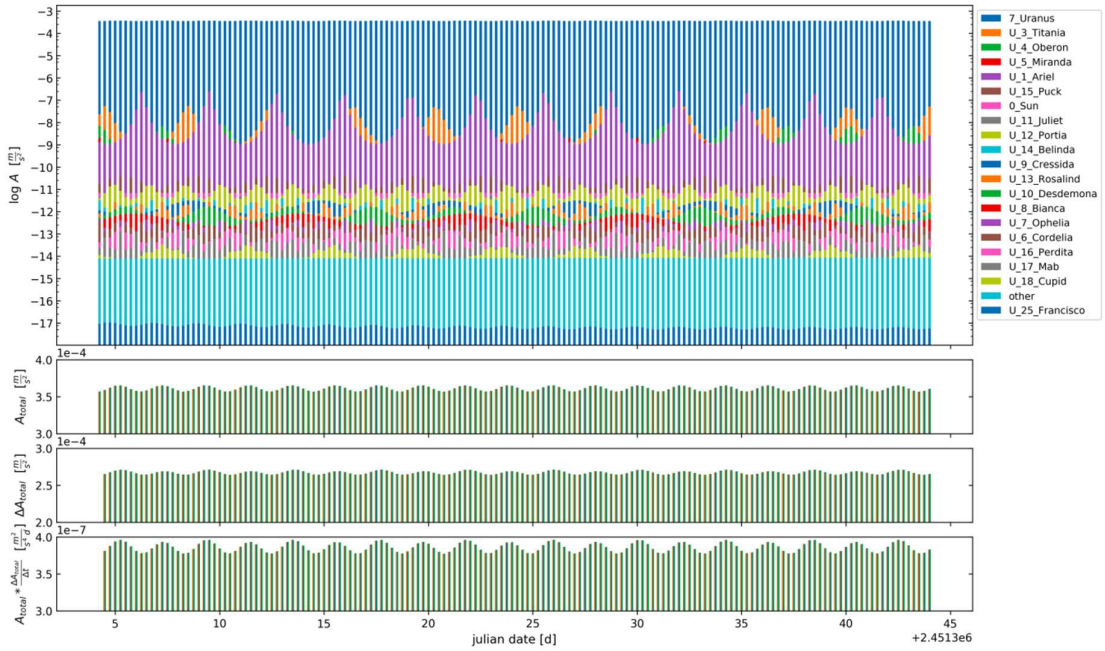

Figure 9. Tidal accelerations acting on Uranian moon Umbriel using the version of the simulation with full orbital elements; Δt = 0.25 days. A denotes the individual tidal accelerations caused by other objects. The ordering of the legend is the same as in the uppermost plot with the strongest contribution at the top and the weakest at the bottom. A_{total} denotes the norm of the vector addition of all individual contributions. ΔA_{total} denotes the norm of the vector difference of A_{total} for two consecutive time steps.

A well investigated extrasolar planetary system is TRAPPIST-1, an M-dwarf with seven exoplanets, the largest extrasolar planetary system found so far. Since all planets are orbiting very close to each other and their host star, this system is of great interest and a challenging example for our approach concerning tidal interactions and consequences especially for tidal heating. Figure 10 shows tidal accelerations for the innermost planet TRAPPIST-1b which even exceed the values found for the Jovian moon (J1) Io, the most strongly tidally influenced object in the solar system. Equally the planets on outer orbits show values in the same range (not shown). We may therefore assume strong to very strong tidal heating and consequently siliceous volcanism may be present if we refer to the relations of Figure 6. This is in good agreement with results in other publications, e.g. [34], confirming an applicability of our model to extrasolar planetary systems. Additionally, the individual tidal influences of all other planets are also visible. The influence of TRAPPIST-1c alone would be enough to periodically exert tidal forces on TRAPPIST-1b up to a lower limit from which on tidal heating of low-melting liquids might already be considered. As M-dwarfs often possess extremely strong magnetic fields another source for heat induction has to be considered [35]. Adding up stored accretion energy, radioactive, tidal and induction heating, this gives an impression of the planets of TRAPPIST-1 as volcanic worlds. An overview and classification in relation to objects in the solar system is given in Figure 6.

For better comparison, we calculate the values of $\{A_{total} \cdot (\Delta A_{total} / \Delta t)\}_{max}$ found in our model using full parameters for (J1) Io, Ganymede and all planets in the TRAPPIST-1 system (Table 1). We chose (J1) Io and Ganymede, because their semi-major axes a are similar to them of the planets in the TRAPPIST-1 system and Jupiter as the object being orbited by (J1) Io and Ganymede is with its huge mass most comparable to the M-dwarf.

Preprints (www.preprints.org) | NOT PEER-REVIEWED | Posted: 19 July 2021 doi:10.20944/preprints202107.0408.v1

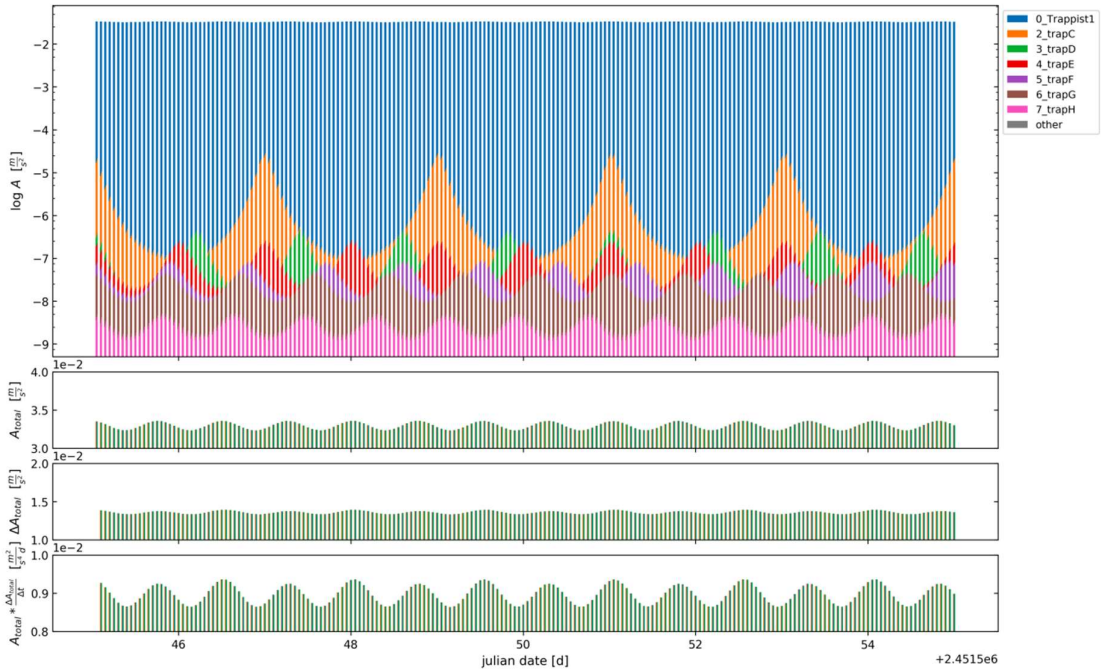

Figure 10. Tidal accelerations acting on exoplanet TRAPPIST-1b using the version of the simulation with full orbital elements (without the longitude of the ascending node Ω, the argument of periapsis ω and the mean anomaly at a given epoch M_0, since no data is available); Δt = 0.05 days. A denotes the individual tidal accelerations caused by other objects. The ordering of the legend is the same as in the uppermost plot with the strongest contribution at the top and the weakest at the bottom. A_{total} denotes the norm of the vector addition of all individual contributions. ΔA_{total} denotes the norm of the vector difference of A_{total} for two consecutive time steps.

Table 1. Comparison of values of $\{A_{total} \cdot (\Delta A_{total} / \Delta t)\}_{max}$ for all planets in the TRAPPIST-1 system and for (J1) Io and Ganymede.

object	a [km]	e	n [rad/day]	R [km]	M [kg]	$A_{total} \cdot (\Delta A_{total} / \Delta t)$ [m²/s⁴d]
TRAPPIST-1b	1.73E+06	0.0062	4.1586	7149.85	6.08E+24	9.36E-03
TRAPPIST-1c	2.37E+06	0.0065	2.5944	6984.02	6.91E+24	8.50E-04
(J1) Io	4.22E+05	0.0041	3.5516	1821.60	8.93E+22	2.43E-04
TRAPPIST-1d	3.33E+06	0.0084	1.5514	5000.43	1.77E+24	3.36E-05
TRAPPIST-1e	4.38E+06	0.0051	1.0302	5804.07	4.61E+24	5.70E-06
TRAPPIST-1f	5.76E+06	0.0101	0.6825	6671.49	5.58E+24	9.98E-07
Ganymede	1.07E+06	0.0013	0.8782	2631.20	1.48E+23	5.24E-07
TRAPPIST-1g	7.01E+06	0.0021	0.5086	7322.06	6.86E+24	2.62E-07
TRAPPIST-1h	9.27E+06	0.0057	0.3348	4930.27	1.98E+24	1.50E-08

4. Discussion

As a "gold standard" system, the simulation approach for tidal accelerations presented here using a minimalistic set of parameters was applied to all objects in our solar system known and correlated to cryo- or even siliceous volcanism. For celestial bodies known to show signs of strong tidal influence, the resulting values for $\{A_{total} \cdot (\Delta A_{total} / \Delta t)\}_{max}$ are among the largest occurring in this simulation. Furthermore, additional objects were suggested which have not been subjects of research for tidal heating up to now.

The identification of new candidates can also reveal conclusions about the composition and evolution of other properties not related to tidal heating, e.g., the inner Neptunian moon Despina shows the highest tidal acceleration value of all objects included in the simulation of the solar system (see Figure 6). According to [36], the composition of

Despina and the other inner Neptunian moons should be structured like a rubble pile, i.e. a loose aggregation of small rocky pieces. Considering the strong tidal forces presumably associated with the relatively high tidal accelerations acting on Despina, it may be interesting to investigate whether or even how rubble piles exposed to such relative strong tidal forces are stable over the long history of the solar system. So, this could lead to new insights into the stability of rubble piles or motivate new ideas about the inner composition of these objects.

As may have been noticed in Figure 5, the Earth shows siliceous volcanism although the tidal accelerations are quite low compared to (J1) Io, the only other object in the solar system for which this persistent characteristic is confirmed. This can be explained with the fact, that due to the huge radius of Earth, accretion heat from the period of formation and radioactive heating contribute more to the occurrence of volcanism on Earth than tidal heating. This also illustrates the need for awareness and consideration of other influences not covered just by tidal acceleration or tidal heating. Nevertheless, this is not a contradiction to our approach. In Figures 6 and 7 one can easily distinguish two main domains: Big objects like our Earth appear at the far-right margin of the plots at large radii R, implying huge contributions from radioactive decay and stored accretion energy. The other domain are tidally interesting objects, appearing at the top in the center and the left margin of the plots with small to intermediate radii R, but large tidal accelerations. Therefore, this domain is the interesting one for tidal heating as the main contribution. Accretion heat and radioactive heating should be minor. All the objects considered as interesting ones in our study can be found in this domain. It can be divided into two sub-domains: The top center contains the already well-known objects in the context of (cryo-)volcanism and tidal heating.

Planets in TRAPPIST-1 system have been taken to test and verify but also to show the limits and borders of this model. The objects are already quote big in comparison with considered objects in the solar system, but they are until now the only set of exoplanets well enough characterized by other models to serve as check-up for our model. Planets of TRAPPIST-1 should experience strong heating by remaining accretion heat, radioactive heating, and tidal heating all together. Hence, planets of TRAPPIST-1 appear to be very hot worlds. This is in concordance with the conclusions from other simulations [37-39].

Future investigations might try to apply this simulation approach to depict perturbations regarding ΔA. It may be an aim to make long-term predictions about the stability and resonances of multi-body systems, since the mutual perturbations of the objects in an energetically relaxed state are visible (energy included in eccentricities dissipated to zero).

Furthermore, simulations without the central object might be desirable to investigate only the mutual tidal influences of the orbiting objects. As already mentioned, this will show that also other objects orbiting the central object can provide the leading important tidal influence (see, e.g., bottom panel of Figure 9 for Umbriel). This may justify our complex multi-body approach.

Some new objects of interest were found and may reason further investigations. The testing on how strong the values change when some parameters are missing yields stable/similar results in the solar system. This encourages the application in extrasolar planetary system to evaluate less well-known objects. The transfer to the extrasolar planetary system TRAPPIST-1 also results in assumptions on the planets being in concordance with known simulations [37-39]. This confirms our choice of TRAPPIST-1 for verification that our model is applicable to extrasolar planetary systems. This might be encouraging to use this approach on further extrasolar systems.

Author Contributions: Conceptualization, G.H.; methodology, K.P. and G.H.; software, K.P.; validation, K.P., A.R. and G.H.; formal analysis, K.P.; investigation, K.P., A.R. and G.H.; resources, M.H. and G.H.; data curation, K.P.; writing—original draft preparation, K.P.; writing—review and

editing, A.R., M.H. and G.H.; visualization, K.P.; supervision, M.H. and G.H.; All authors have read and agreed to the published version of the manuscript.

Funding: This research received no external funding

Acknowledgments: The authors thank Margot Chazotte, Aaron Sievers, Andrea Zanna and Silvia Zanna for stylistic review of the manuscript.

Conflicts of Interest: The authors declare no conflict of interest.

Appendix A

This appendix contains details and resources of data.

Table 2. Resources of data for TNOs. If several value sources for one object were available, we use the mean value of these data. In the column 'moons' an asterisk (*) denotes that a moon is known for this TNO but not included in the simulation because of missing or inaccurate data.

TNO	Radius	mass	orbital elements	moons
(19521) Chaos (1998 WH24)	[40]			
(38628) Huya (2000 EB173)	[40]			
(47171) Lempo (1999 TC36)	[40]	[41]		
(50000) Quaoar (2002 LM60)	[40, 42]	[42, 43]		*
(58534) Logos (1997 CQ29)	[44]	[44]		*
(65489) Ceto (2003 FX128)	[40]	[45]		*
(66652) Borasisi (1999 RZ253)	[40]	[46]		*
(88611) Teharonhiawako (2001 QT297)	[40]	[46]		*
(90377) Sedna (2003 VB12)	[40]			
(90482) Orcus (2004 DW)	[40]	[47]		*
(120347) Salacia (2004 SB60)	[40]	[40, 48]		*
(136108) Haumea	[40, 49, 50]			Namaka, Hi'iaka
(136199) Eris (2003 UB313)	[51]	[52]		Dysnomia
(136472) Makemake (2005 FY9)	[50, 53]			*
(148780) Altjira (2001 UQ18)	[40]	[40]		
(174567) Varda (2003 MW12)	[40]	[54]		*
(136199) Eris I Dysnomia	[12]	[12]	[52]	
(136108) Haumea II Namaka	[12]	[12]	[49]	
(136108) Haumea I Hi'iaka	[12]	[12]	[49]	

References

1. Dressing, C. D.; Charbonneau, D. The occurrence rate of small planets around small stars. *Astrophysical Journal, 767(1),* **2013,** 95.
2. Gillon, M.; Jehin, E.; Lederer, S. M.; Delrez, L.; de Wit, J.; Burdanov, A.; van Grootel, V.; Burgasser, A. J.; Triaud, A. H. M. J.; Opitom, C.; Demory, B. O.; Sahu, D. K.; Bardalez Gagliuffi, D.; Magain, P.; Queloz, D. Temperate Earth-sized planets transiting a nearby ultracool dwarf star. *Nature, 533(7602),* **2016,** 221–224.
3. Gillon, M.; Triaud, A. H. M. J.; Demory, B. O.; Jehin, E.; Agol, E.; Deck, K. M.; Lederer, S. M.; de Wit, J.; Burdanov, A.; Ingalls, J. G.; Bolmont, E.; Leconte, J.; Raymond, S. N.; Selsis, F.; Turbet, M.; Barkaoui, K.; Burgasser, A.; Burleigh, M. R.; Carey, S. J.; Chaushev, A.; Copperwheat, C. M.; Delrez, L.; Fernandes, C. S.; Holdsworth, D. L.; Kotze, E. J.; Van Grootel, V.; Almleaky, Y.;

Benkhaldoun, Z.; Magain, P.; Queloz, D. Seven temperate terrestrial planets around the nearby ultracool dwarf star TRAPPIST-1. *Nature, 542(7642),* **2017,** 456–460.

4. Jet Propulsion Laboratory (JPL), California Institute of Technology (Caltech) and National Araeronatics and Space Agengy (NASA) (1996a) Solar System Bodies [database]. Retrieved from: https://ssd.jpl.nasa.gov/?bodies.
5. Jet Propulsion Laboratory (JPL), California Institute of Technology (Caltech) and National Araeronatics and Space Agengy (NASA) (1996b) JPL Small-Body Database Search Engine [database]. Retrieved from https://ssd.jpl.nasa.gov/sbdb_query.cgi.
6. Steadly, R. S.; Robinson, M. S. *The Astronomical Almanac for the Year 2012: Data for Astronomy, Space Sciences, Geodesy, Surveying, Navigation and other Applications.* U.S. Government Printing Office, 2012.
7. Van Grootel, V.; Fernandes, C. S.; Gillon, M.; Jehin, E.; Manfroid, J.; Scuflaire, R.; Burgasser, A. J., Barkaoui, K.; Benkhaldoun, Z.; Burdanov, A.; Delrez, L.; Demory, B.-O.; de Wit, J.; Queloz, D.; Triaud, A. H. M. J. Stellar Parameters for Trappist-1, The Astrophysical Journal. *IOP Publishing, 853(1),* **2018,** 30.
8. Grimm, S. L.; Demory, B.-O.;, Gillon, M.; Dorn, C.; Agol, E.; Burdanov, A.; Delrez, L.; Sestovic, M.; Triaud, A. H. M. J.; Turbet, M.; Bolmont, É.; Caldas, A.; de Wit, J.; Jehin, E.; Leconte, J.; Raymond, S. N.; Van Grootel, V.; Burgasser, A. J.; Carey, S.; Fabrycky, D.; Heng, K.; Hernandez, D. M.; Ingalls, J. G.; Lederer, S.; Selsis, F.; Queloz, D. The nature of the TRAPPIST-1 exoplanets, Astronomy & Astrophysics. *EDP Sciences, 613,* **2018,** A68.
9. Delrez, L.; Gillon, M.; Triaud, A. H. M. J.; Demory, B.-O.; de Wit, J.; Ingalls, J. G.; Agol, E.; Bolmont, E.; Burdanov, A.; Burgasser, A. J.; Carey, S. J.; Jehin, E.; Leconte, J.; Lederer, S.; Queloz, D.; Selsis, F.; Van Grootel, V. Early 2017 observations of TRAPPIST-1 with Spitzer, Monthly Notices of the Royal Astronomical Society. Oxford University Press, 475(3), **2018,** pp. 3577–3597.
10. Gillon, M.; Triaud, A. H. M. J.; Demory, B.-O.; Jehin, E.; Agol, E.; Deck, K. M.; Lederer, S. M.; de Wit, J.; Burdanov, A.; Ingalls, J. G.; Bolmont, E.; Leconte, J.; Raymond, S. N.; Selsis, F.; Turbet, M.; Barkaoui, K.; Burgasser, A.; Burleigh, M. R.; Carey, S. J.; Chaushev, A.; Copperwheat, C. M.; Delrez, L.; Fernandes, C. S.; Holdsworth, D. L.; Kotze, E. J.; Van Grootel, V.; Almleaky, Y.; Benkhaldoun, Z.; Magain, P.; Queloz, D. Seven temperate terrestrial planets around the nearby ultracool dwarf star TRAPPIST-1, *Nature 542(7642),* **2017,** 456–460.
11. Guennebaud, G., Jacob, B. and others (2010) Eigen v3 [C++ library]. Retrieved from http://eigen.tuxfamily.org.
12. Saxena, P.; Renaud, J. P.; Henning, W. G.; Jutzi, M.; Hurforda, T. Relevance of tidal heating on large TNOs, *Icarus 302,* **2018,** 245–260.
13. Hanson, B. Mercury, up-close again. Introduction, Science (New York, N.Y.). American Association for the Advancement of *Science, 321(5885),* **2008,** 58.
14. Head, J. W.; Chapman, C. R.; Strom, R. G.; Fassett, C. I.; Denevi, B. W.; Blewett, D. T.; Ernst, C. M.; Watters, T. R.; Solomon, S. C.; Murchie, S. L.; Prockter, L. M.; Chabot, N. L.; Gillis-Davis, J. J.; Whitten, J. L.; Goudge, T. A.; Baker, D. M. H.; Hurwitz, D. M.; Ostrach, L. R.; Xiao, Z.; Merline, W. J.; Kerber, L.; Dickson, J. L.; Oberst, J.; Byrne, P. K.; Klimczak, C.; Nittler, L. R. Flood volcanism in the northern high latitudes of Mercury revealed by MESSENGER, Science (New York, N.Y.). *American Association for the Advancement of Science, 333(6051),* **2011,** 1853–1856.
15. Shalygin, E. V.; Markiewicz, W. J.; Basilevsky, A. T.; Titov, D. V.; Ignatiev, N. I.; Head, J. W. Active volcanism on Venus in the Ganiki Chasma rift zone, *Geophysical Research Letters 42(12),* **2015,** 4762–4769.
16. Armann, M.; Tackley, P. J. Simulating the thermochemical magmatic and tectonic evolution of Venus's mantle and lithosphere: Two-dimensional models, *Journal of Geophysical Research: Planets, 117(E12),* **2012.**
17. Ulmschneider, P. Intelligent life in the universe: principles and requirements behind its emergence. Springer-Verlag, **2006.**
18. Scholz, M. Astrobiologie. Berlin, Heidelberg: Springer Berlin Heidelberg, **2016.**
19. Mikhail, S.; Heap, M. J. Hot climate inhibits volcanism on Venus: Constraints from rock deformation experiments and argon isotope geochemistry, *Physics of the Earth and Planetary Interiors, 268,* **2017,** 18–34.
20. Spudis, P. D. Chapter 39 - Volcanism on the Moon, The Encyclopedia of Volcanoes (Second Edition). Academic Press, **2015,** pp. 689–700.
21. Weber, R. C.; Lin, P.-Y., Garnero, E. J.; Williams, Q.; Lognonné, P. Seismic detection of the lunar core, Science (New York, N.Y.). *American Association for the Advancement of Science, 331(6015),* **2011,** 309–312.
22. Anderson, J. D.; Schubert, G.; Jacobson, R. A.; Lau, E. L.; Moore, W. B.; Sjogren, W. L. Europa's differentiated internal structure: inferences from four Galileo encounters., Science (New York, N.Y.). *American Association for the Advancement of Science, 281(5385),* **1998,** 2019–2022.
23. Vance, S.; Bouffard, M.; Choukroun, M.; Sotin, C. Ganymede's internal structure including thermodynamics of magnesium sulfate oceans in contact with ice, *Planetary and Space Science, 96,* **2014,** 62–70.
24. Showman, A. P.; Malhotra, R. The Galilean satellites, Science (New York, N.Y.). *American Association for the Advancement of Science, 286(5437),* **1999,** 77–84.
25. Hansen, C. J.; Esposito, L.; Stewart, A. I. F.; Colwell, J.; Hendrix, A.; Pryor, W.; Shemansky, D.; West, R. Enceladus' water vapor plume, Science (New York, N.Y.). *American Association for the Advancement of Science, 311(5766),* **2006,** 1422–1425.
26. Grasset, O.; Sotin, C.; Deschamps, F. On the internal structure and dynamics of Titan, *Planetary and Space Science, 48(7–8),* **2000,** 617–636.

27. Beuthe, M.; Rivoldini, A.; Trinh, A. Enceladus's and Dione's floating ice shells supported by minimum stress isostasy, Geophysical Research, **2016**.
28. Hussmann, H.; Sohl, F.; Spohn, T. Subsurface oceans and deep interiors of medium-sized outer planet satellites and large trans-neptunian objects, *Icarus, 185(1),* **2006,** 258–273.
29. Tittemore, W. C.; Wisdom, J. Tidal evolution of the Uranian satellites: III. Evolution through the Miranda-Umbriel 3:1, Miranda-Ariel 5:3, and Ariel-Umbriel 2:1 mean-motion commensurabilities, *Icarus, 85(2),* **1990,** 394–443.
30. Bergstralh, J. T.; Miner, E. D.; Matthews, M. S. Uranus. University of Arizona Press, **1991.**
31. Ruesch, O.; Platz, T.; Schenk, P.; McFadden, L. A.; Castillo-Rogez, J. C.; Quick, L. C.; Byrne, S.; Preusker, F.; O'Brien, D. P.; Schmedemann, N.; Williams, D. A.; Li, J.-Y.; Bland, M. T.; Hiesinger, H.; Kneiss, T.; Neesemann, A.; Schaefer, M.; Pasckert, J. H.; Schmidt, B. E.; Buczkowski, D. L.; Sykes, M. V.; Nathues, A.; Roatsch, T.; Hoffmann, M.; Raymond, C. A.; Russell, C. T. Cryovolcanism on Ceres, Science (New York, N.Y.). *American Association for the Advancement of Science, 353(6303),* **2016,** aaf4286.
32. Desch, S. J.; Cook, J. C.; Doggetta, T.C.; Portera, S. B. Thermal evolution of Kuiper belt objects, with implications for cryovolcanism, *Icarus, 202(2),* **2009,** 694–714.
33. Dumas, C.; Carry, B.; Hestroffer, D.; Merlin, F. High-contrast observations of (136108) Haumea, Astronomy & Astrophysics. EDP Sciences, 528, **2011,** p. A105.
34. Barr, A. C.; Dobos, V.; Kiss, L. L. Interior structures and tidal heating in the TRAPPIST-1 planets, Astronomy & Astrophysics. EDP Sciences, 613, **2018,** p. A37.
35. Kislyakova, K. G.; Noack, L.; Johnstone, C. P.; Zaitsev, V. V.; Fossati, L.; Lammer, H.; Khodachenko, M. L.; Odert, P.; Güdel, M. Magma oceans and enhanced volcanism on TRAPPIST-1 planets due to induction heating, *Nature Astronomy, 1(12),* **2017,** 878–885.
36. Banfield, D.; Murray, N. A dynamical history of the inner Neptunian satellites, *Icarus, 99(2),* **1992,** 390–401.
37. Barr, A. C., Dobos, V., & Kiss, L. L. Interior structures and tidal heating in the TRAPPIST-1 planets. *Astronomy and Astrophysics, 613,* **2018,** 37.
38. Dobos, V., Barr, A. C., & Kiss, L. L. Tidal heating and the habitability of the TRAPPIST-1 exoplanets. *Astronomy and Astrophysics, 624,* **2019,** A2.
39. Hay, H. C. F. C., & Matsuyama, I. Tides Between the TRAPPIST-1 Planets. *The Astrophysical Journal, 875(1),* **2019**, 22.
40. Vilenius, E.; Kiss, C.; Mommert, M.; Müller, T.; Santos-Sanz, P.; Pal, A.; Stansberry, J.; Mueller, M.; Peixinho, N.; Fornasier, S.; Lellouch, E.; Delsanti, A.; Thirouin, A.; Ortiz, J. L.; Duffard, R.; Perna, D.; Szalai, N.; Protopapa, S.; Henry, F.; Hestroffer, D.; Rengel, M.; Dotto, E.; Hartogh, P. "TNOs are Cool": A survey of the trans-Neptunian region, Astronomy & Astrophysics. EDP Sciences, 541(A94), **2012.**
41. Benecchi, S. D.; Noll, K. S.; Grundy, W. M.; Levison, H. F. (47171) 1999 TC36, A transneptunian triple, *Icarus, 207(2),* **2010,** 978–991.
42. Braga-Ribas, F.; Sicardy, B.; Ortiz, J. L.; Lellouch, E.; Tancredi, G.; Lecacheux, J.; Vieira-Martins, R.; Camargo, J. I. B.; Assafin, M.; Behrend, R.; Vachier, F.; Colas, F.; Morales, N.; Maury, A.; Emilio, M.; Amorim, A.; Unda-Sanzana, E.; Roland, S.; Bruzzone, S.; Almeida, L. A.; Rodrigues, C. V.; Jacques, C.; Gil-Hutton, R.; Vanzi, L.; Milone, A. C.; Schoenell, W.; Salvo, R.; Almenares, L.; Jehin, E.; Manfroid, J.; Sposetti, S.; Tanga, P.; Klotz, A.; Frappa, E.; Cacella, P.; Colque, J. P.; Neves, C.; Alvarez, E. M.; Gillon, M.; Pimentel, E.; Giacchini, B.; Roques, F.; Widemann, T.; Magalhães, V. S.; Thirouin, A.; Duffard, R.; Leiva, R.; Toledo, I.; Capeche, J.; Beisker, W.; Pollock, J.; Cedeño Montaña, C. E.; Ivarsen, K.; Reichart, D.; Haislip, J.; Lacluyze, A. The size, shape, albedo, density, and atmospheric limit of transneptunian object (50000) quaoar from multi-chord stellar occultations. *The Astrophysical Journal, 773(1),* **2013,** 26.
43. Fraser, W. C.; Batygin, K.; Brown, M. E.; Bouchez, A. The mass, orbit, and tidal evolution of the Quaoar–Weywot system, *Icarus, 222(1),* **2013,** 357–363.
44. Grundy, W. M.; Noll, K. S.; Stephens, D. C. Diverse albedos of small trans-neptunian objects, *Icarus, 176(1),* **2005,** 184–191.
45. Grundy, W. M.; Stansberry, J.A.; Noll, K.S.; Stephens, D.C.; Trilling, D.E.; Kern, S.D.; Spencer, J.R.; Cruikshank, D.P.; Levison, H.F. The orbit, mass, size, albedo, and density of (65489) Ceto/Phorcys: A tidally-evolved binary Centaur, *Icarus, 191(1),* **2007,** 286–297.
46. Grundy, W. M.; Noll, K.S.; Nimmo, F.; Roe, H.G.; Buie, M.W.; Porter, S.B.; Benecchi, S.D.; Stephens, D.C.; Levison, H.F.; Stansberry, J.A. Five new and three improved mutual orbits of transneptunian binaries, *Icarus, 213(2),* **2011,** 678–692.
47. Carry, B.: Hestroffer, D.; DeMeo, F. E.; Thirouin, A.; Berthier, J.; Lacerda, P.; Sicardy, B.; Doressoundiram, A.; Dumas, C.; Farrelly, D.; Müller, T. G. Integral-field spectroscopy of (90482) Orcus-Vanth, Astronomy & Astrophysics. EDP Sciences, 534, **2011,** A115.
48. Stansberry, J. A.; Grundy, W.M.; Mueller, M.; Benecchi, S.D.; Rieke, G.H.; Noll, K.S.; Buie, M.W.; Levison, H.F.; Porter, S.B.; Roe, H.G. Physical properties of trans-neptunian binaries (120347) Salacia–Actaea and (42355) Typhon–Echidna, *Icarus, 219(2),* **2012,** 676–688.
49. Ragozzine, D.; Brown, M. E. Orbits and masses of the satellites of the dwarft planet Humea (2003 EL61), *The Astronomical Journal 137(6),* **2009,** 4766–4776.

50. Ortiz, J. L.; Sicardy, B.; Braga-Ribas, F.; Alvarez-Candal, A.; Lellouch, E.; Duffard, R.; Pinilla-Alonso, N.; Ivanov, V. D.; Littlefair, S. P.; Camargo, J. I. B.; Assafin, M.; Unda-Sanzana, E.; Jehin, E.; Morales, N.; Tancredi, G.; Gil-Hutton, R.; de la Cueva, I.; Colque, J. P.; Da Silva Neto, D. N.; Manfroid, J.; Thirouin, A.; Gutiérrez, P. J.; Lecacheux, J.; Gillon, M.; Maury, A.; Colas, F.; Licandro, J.; Mueller, T.; Jacques, C.; Weaver, D.; Milone, A.; Salvo, R.; Bruzzone, S.; Organero, F.; Behrend, R.; Roland, S.; Vieira-Martins, R.; Widemann, T.; Roques, F.; Santos-Sanz, P.; Hestroffer, D.; Dhillon, V. S.; Marsh, T. R.; Harlingten, C.; Campo Bagatin, A.; Alonso, M. L.; Ortiz, M.; Colazo, C.; Lima, H. J. F.; Oliveira, A. S.; Kerber, L. O.; Smiljanic, R.; Pimentel, E.; Giacchini, B.; Cacella, P.; Emilio, M. Albedo and atmospheric constraints of dwarf planet Makemake from a stellar occultation, *Nature, 491(7425),* **2012,** 566–569.
51. Sicardy, B.; Ortiz, J. L.; Assafin, M.; Jehin, E.; Maury, A.; Lellouch, E.; Gil-Hutton, R.; Braga-Ribas, F.; Colas F.; Lecacheux, J.; Roques, F.; Santos-Sanz, P.; Widemann, T.; Morales, N.; Thirouin, A.; Camargo, J. I. B.; Vieira-Martins, R.; Gillon, M.; Manfroid, J.; Behrend, R.; the Eris occultation team. Size, density, albedo and atmosphere limit of dwarf planet Eris from a stellar occultation, EPSC Abstracts. European Planetary Science Congress - Division for Planetary Sciences (EPSC-DPS) Joint Meeting 2011, 6(EPSC-DPS2011-137-8). Available online at: http://meetingorganizer.copernicus.org/EPSC-DPS2011/EPSC-DPS2011-137-8.pdf.
52. Brown, M. E.; Schaller, E. L. The Mass of Dwarf Planet Eris, *Science, 316(5831),* **2007**, 1585 LP-1585.
53. Brown, M. E. On the size, shape, and density of dwarf planet Makemake. *The Astrophysical Journal, 767(1),* **2013,** L7.
54. Grundy, W. M.; Porter, S.B.; Benecchi, S.D.; Roe, H.G.; Noll, K.S.; Trujillo, C.A.; Thirouin, A.; Stansberry, J.A.; Barker, E.; Levison, H.F. The Mutual Orbit, Mass, and Density of the Large Transneptunian Binary System Varda and Ilmarë, *Icarus, 257,* **2015**, 130-138.